Supporting Information for "Decadal variability of ice-shelf melting in the Amundsen Sea driven by sea-ice freshwater fluxes"

Michael Haigh[1]& Paul R. Holland[1]

[1]British Antarctic Survey, Cambridge, UK

Contents of this file

1. Text S1 to S4
2. Figures S1 to S4

Introduction

In this document we present additional output of the regional model used in this study. Fig. S1, which is discussed in Text S1, shows the time-mean and composites (using the undercurrent as the predictor) of the surface stress curl in the regional model. The data shown in this figure suggest that the surface stress curl is not responsible for driving the diagnosed decadal variability in the undercurrent and ice shelf melt.

We also present outputs of an idealised model used to reproduce the mechanism by which freshwater fluxes drive decadal variability of the Amundsen Sea undercurrent. The idealised model setup is shown in Fig. S2 and discussed in Text S2. The idealised model output is shown in Fig. S3 and discussed in Text S3.

Text S1

Silvano et al. (2022) presented model results showing that variability of the eastward undercurrent at the Amundsen Sea shelf break opposes variability of the surface winds on decadal timescales. For example, eastward wind anomalies typically coincide with a slower undercurrent. Silvano et al. (2022) hypothesised that this was due to on-shelf wind stress curl variability producing Ekman upwelling and downwelling anomalies that raise and lower isopycnals on the continental shelf. The suggestion was then that this leads to baroclinic anomalies at the shelf break that outweigh the barotropic effects of the shelf-break winds. In this section we consider the surface stress curl outputted by the ocean model used in this study, which accounts for sea ice and ocean currents.

Fig. S1a shows the time-mean surface stress curl, while Figs. S1b,c show composite anomaly responses of the surface stress curl using the undercurrent as predictor. These composites exhibit little clear spatial dependence, and do not obviously imply the existence of a physical link between the surface stress curl and the undercurrent. We may average the surface stress curl over the continental shelf (over the shelf region shown in Fig 3a of the main text) to ascertain whether, on average, the wind stress curl has the sign required for it to be the driver of the diagnosed decadally varying baroclinicity. For eastward undercurrent anomalies, during which cross-slope baroclinicity is large, we find that the sign of the area-averaged on-shelf anomaly is opposite to that required. That is, on average, the associated Ekman velocity anomaly is upward, which would be expected to raise on-shelf isopycnals and reduce the cross-shelf break baroclinicity. This leads us to conclude that surface stress curl variability is not responsible for the decadal variability of the undercurrent. Instead, results that we present in the main text show that sea-ice and ice-shelf freshwater fluxes are responsible.

Text S2

In this section we utilise the MITgcm configuration introduced by Haigh, Holland, and Jenkins (2023) to simulate the mechanism by which freshwater fluxes drive undercurrent variability in an idealised configuration. The model includes no ice shelves, sea ice or icebergs. This model uses a highly simplified forcing and geometry, summarised in Fig. S2. The domain (Fig. S2a) is a zonally re-entrant channel with continental shelf bathymetry which is 1000 m deep in the north and 500 m deep in the south, separated by a steep continental shelf slope. Walls on the continental shelf outline an embayment similar to the real Amundsen Sea. On the eastern side of the shelf slope we include a 700 m-deep trough and to its east a 400 m-deep ridge. As discussed in Haigh et al. (2023), these bathymetric features help to induce a deep cyclonic circulation on the continental shelf, as is simulated in the regional model.

The model is forced by a steady wind (Fig. S2a) that is motivated by actual time-mean winds over the Amundsen Sea. The wind is westerly (easterly) to the north (south) of the continental shelf break, and zero above the continental shelf slope. The wind speed extrema of 4 m s^{-1} is attained at the northern and southern boundaries.

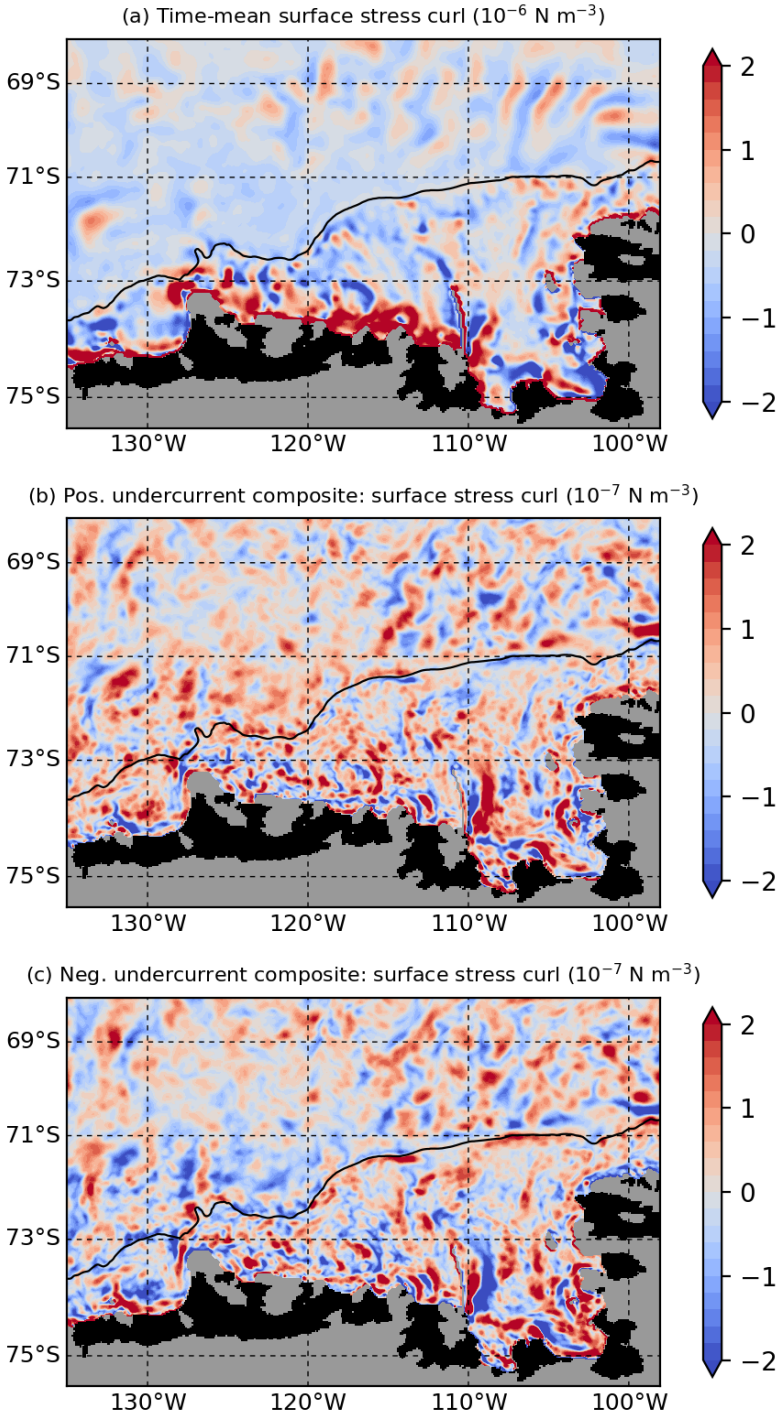

Figure S1. (a) Time-mean surface stress curl (10^{-6} N m^{-3}). (b,c) Composites of surface stress curl anomaly (10^{-7} N m^{-3}) for eastward/westward undercurrent anomalies. In all panels, grey masking represents land, black masking represents the ice shelves, and the black contour represents the 1000 m shelf-break isobath.

Potential temperature θ and salinity S are relaxed at the northern and southern boundaries to the profiles shown in Fig. S2c. At the northern boundary the relaxation profile includes a thermocline/halocline between 100 m and 300 m depths, which separates cold and fresh surface waters from warm and saline deep waters (CDW).

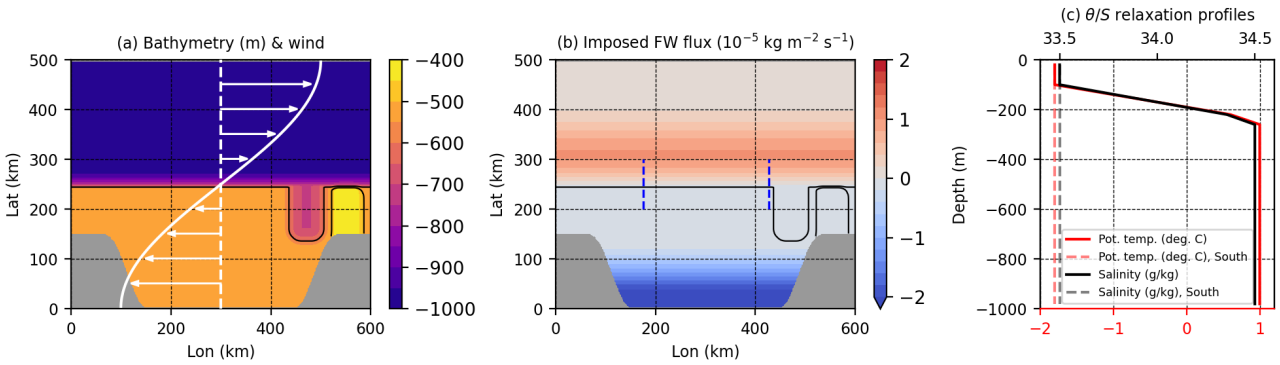

Figure S2. Setup of the idealised model. (a) Idealised model bathymetry (colour, m). Black contours represent the 500 m and 600 m isobaths. White arrows and contour represent the steady zonally uniform zonal wind measured relative to the white dashed line. The wind speed is zero over centre of the continental slope and is fastest with speed ± 4 m s^{-1} at the northern/southern boundary. (b) Spatial distribution of surface freshwater flux forcing (10^{-5} kg m^{-2} s^{-1}), which oscillates with 10-year period. This represents a time-mean evaluated over one positive phase of the forcing. (c) Relaxation profiles for potential temperature, θ (red), and salinity, S (black). Solid lines represent the profiles applied at the northern boundary with 10-day timescale and dashed lines represent the profiles applied at the southern boundary with 200-day timescale.

The timescale for the relaxation at the northern boundary is 10 days. At the southern boundary (Lat = 0 km) θ and S are relaxed towards -1.8°C and 33.5 g kg^{-1}, respectively. These values are also taken for the cold and fresh initial conditions used in model runs. At the southern boundary a 200-day relaxation timescale is used, significantly weaker than the relaxation at the northern boundary. This weak relaxation at the southern boundary is required for the model to maintain a realistic on-shelf heat distribution and realistic ASF at the shelf slope in steady state, since otherwise the shelf properties gradually drift warmer on centennial timescales. Haigh et al. (2023) found that wind-driven coastal downwelling at the southern boundary is not sufficient to maintain the ASF on these long timescales. At both the northern and southern boundaries the relaxation is switched off gradually over 4 grid points inward from the boundary.

Forced by the surface winds and θ/S relaxation, the model is spun up from rest for 40 years and is statistically stable after $\sim$ 20 years. The model is then restarted and run for a further 30 years with a freshwater flux applied at the surface which oscillates between positive and negative phases on a 10-year timescale. Fig. S2b shows the surface freshwater flux profile (a time-mean evaluated over the positive phase), which is motivated by composites from the regional model (main text Fig. 2d,f). In its positive phase the surface freshwater flux is positive (freshening) north of the shelf break and is negative (salinification) near the southern coast.

We use this surface flux to show that sea-ice freshwater fluxes alone are sufficient to drive decadal variability in the undercurrent that opposes the surface current. That is, we do not impose any variable ice-shelf melting and by extension we do not include the positive feedback effect that such melting would have on the undercurrent. The winds are held steady throughout the simulation.

Text S3

All output we show here is from the 30-year restart of the idealised model. Data is zonally averaged along the undercurrent section depicted in Fig. S2b. Fig. S3a shows depth-latitude plots of the time-mean density and zonal velocity. The model includes an ASF which is partially maintained by wind-driven downwelling at the southern boundary. A westward slope current sits above the ASF which transitions to an eastward undercurrent beneath the ASF due to thermal wind balance.

Fig. S3d shows timeseries of the along-slope surface current and undercurrent, both with 5-year running mean applied. Also shown is the time-dependence of the applied surface freshwater flux. The surface current and

undercurrent are anticorrelated ($r = -0.60$, 99% significant), with the variable surface freshwater flux driving the same mechanism as in the regional model. The undercurrent response lags the freshwater flux with largest correlations ($r = -0.88$, 99% significant) diagnosed for a 2-year lag.

Fig. S3b,c shows composites of the density and along-slope velocity computed for undercurrent anomalies more than half of a standard deviation from the mean. The effect of the surface freshwater flux on the density is very similar to the regional model. The response to the off-shelf freshwater fluxes is concentrated in the upper 100 m of the water column, whereas the response to the on-shelf freshwater fluxes is spread through the entire 500 m depth. This is likely a consequence of the stratification being stronger off-shelf, which suppresses vertical mixing of salinity between the surface and deeper layers. The on-shelf response is weaker than in the regional model, but the total freshwater flux variability on the shelf is smaller in the idealised model as we do not include the contribution from the ice shelves.

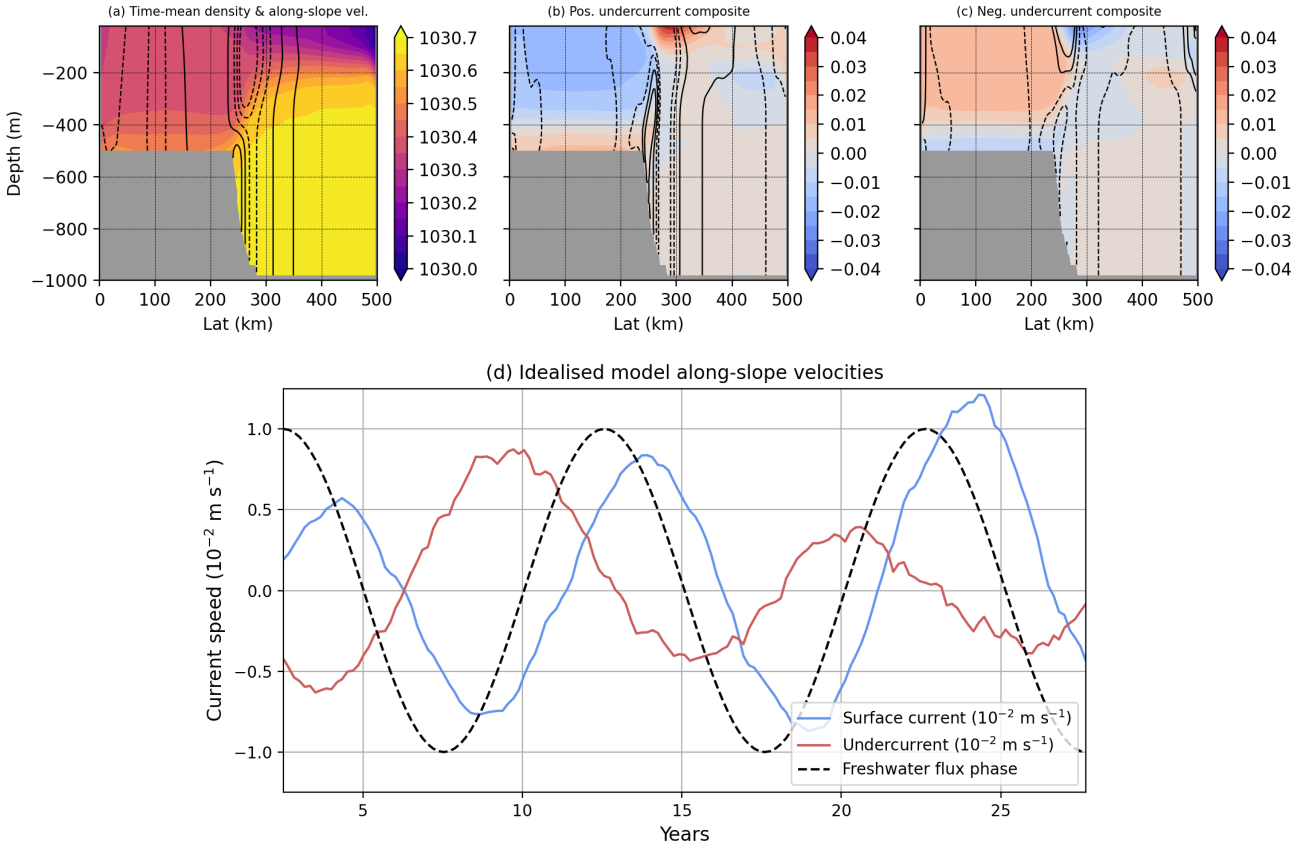

Figure S3. Idealised model outputs. (a) The time-mean, zonal-mean density (colour, kg m^{-3}) and zonal velocity (contours, 0.02 m s^{-1} contour interval). (b) Composites of the density (colour, kg m^{-3}) and zonal velocity (contours, 0.002 m s^{-1} contour interval) anomalies for eastward undercurrent anomalies. (c) The same as (b) but for westward undercurrent anomalies. (d) Timeseries of the surface current (blue, 10^{-2} m s^{-1}), undercurrent (red, 10^{-2} m s^{-1}) and time-dependence of the surface freshwater flux (black dashed). All zonal averages are evaluated along the section shown Fig. S2b. Timeseries have had 5-year running mean applied.

References

Haigh, M., Holland, P. R., & Jenkins, A. (2023, May). The Influence of Bathymetry Over Heat Transport Onto the Amundsen Sea Continental Shelf. *Journal of Geophysical Research: Oceans*, *128*(5). doi: 10.1029/2022jc019460

Silvano, A., Holland, P. R., Naughten, K. A., Dragomir, O., Dutrieux, P., Jenkins, A., ... Naveira Garabato, A. C. (2022, December). Baroclinic Ocean Response to Climate Forcing Regulates Decadal Variability of Ice-Shelf Melting in the Amundsen Sea. *Geophysical Research Letters*, *49*(24). doi: 10.1029/2022gl100646